Available online at www.sciencedirect.com

SciVerse ScienceDirect

Procedia Engineering 00 (2016) 000–000

Procedia Engineering

www.elsevier.com/locate/procedia

1st International Conference on the Material Point Method, MPM 2017

An implicit high-order material point method

Yousef G. Motlagh[a], William M. Coombs[b,*]

[a]*School of Chemical and Process Engineering, University of Leeds, Leeds LS2 9JT, UK*
[b]*School of Engineering and Computing Sciences, Durham University, Science Site, South Road, Durham, DH1 3LE, UK*

Abstract

The material point method (MPM) is a version of the particle-in-cell (PIC) which has substantial advantages over pure Lagrangian or Eulerian methods in numerical simulations of problems involving large deformations. The MPM helps to avoid mesh distortion and tangling problems related to Lagrangian methods and as well as the advection errors associated with Eulerian methods. Despite the MPM being promoted for its ability to solve large deformation problems the method suffers from instabilities when material points cross between elements. These instabilities are due to the lack of smoothness of the grid basis functions used for mapping information between the material points and the background grid. In this paper a novel high-order MPM is developed to eliminate the cell-crossing instability and improve the accuracy of the MPM method.

Peer-review under responsibility of the organizing committee of the 1 st International Conference on the Material Point Method.

Keywords: material point method; B-spline; implicit; quasi-static.

1. Introduction

The material-point method (MPM) is a numerical method for solving continuum problems in fluid and solid mechanics. Its origins are the particle-in-cell (PIC) method developed at Los Alamos in the 1950s [1,2] to model highly distorted fluid flow such as the splash of a falling drop. In the late 1980s, Brackbill and Ruppel [3] revived the PIC technology with simple modifications that reduced the numerical dissipation and made PIC competitive with current technologies for simulating hydrodynamics. The MPM [4–6] is a version of this method that is applicable to solids with strength and stiffness and has been applied to model diverse applications such as impact, penetration, fracture, metal forming, granular media and membranes.

In order to combine the advantages of Eulerian and Lagrangian methods, MPM uses two representations of the continuum. First, MPM discretises a continuum body of fluid or solid with a finite set of material points in the original configuration that are tracked throughout the deformation process. Each material point has a mass, position, velocity and stress, as well as material parameters and internal variables as needed for constitutive models or thermodynamics. These material points provide a Lagrangian description of the material that is not subject to mesh tangling because no connectivity is assumed between the points. The latter description, an Eulerian framework, is an often regular

* Corresponding author.
E-mail address: w.m.coombs@durham.ac.uk

1877-7058
Peer-review under responsibility of the organizing committee of the 1 st International Conference on the Material Point Method.

background mesh that covers the computational domain. Information is transferred from the material points to the background mesh, the equilibrium equations are solved on the background mesh, and then information from the mesh solution used to update the material points, at which time the background mesh can be modified if desired, the cycle then repeats.

Despite the MPM being promoted for its ability to solver large deformation problems it suffers from instabilities when material points cross between elements. These instabilities are due to the lack of smoothness of the grid basis functions used for mapping information between the material points and the background grid. By introducing a weighting function with higher degree of smoothness, the generalized interpolation material point (GIMP) method is capable of reducing these errors and improving accuracy [7]. Convected particle domain interpolation (CPDI) is another algorithm developed to improve the accuracy and efficiency of the material point method for problems involving extremely large tensile deformation and rotation [8]. However, both methods require the basis functions (normally taken to be linear) to be integrated over the domain of the material point of interest, they also do not fully eliminate spurious oscillations due to cell crossing. In this paper an alternative approach is suggested where smooth B-spline function spaces are used to map between the material points and the background grid. The high-order smoothness of the splines eliminates the cell-crossing instability. The remainder of the paper is summarized as follows: in Section 2 we present formulation of the quasi-static material point method. In Section 3 we present our numerical studies for quasi-static material point method, finally conclusions are drawn in Section 4.

2. The quasi-static implicit material point method

Let us start by recalling the elastostatic equations. Let $\Omega \subset \mathbb{R}^d, d = 2, 3$, denote the domain occupied by the body, and let $\Gamma = \partial\Omega$ be its boundary. Then

$$\nabla \cdot \boldsymbol{\sigma} + \boldsymbol{f} = \boldsymbol{0} \quad \text{in } \Omega, \qquad \boldsymbol{u} = \boldsymbol{g} \quad \text{on } \Gamma_D \qquad \text{and} \qquad \boldsymbol{\sigma} \cdot \boldsymbol{n} = \boldsymbol{h} \quad \text{on } \Gamma_N, \tag{1}$$

where $\boldsymbol{\sigma}$ denotes the symmetric Cauchy stress tensor and $\boldsymbol{f}$ is the body force per unit volume, $\boldsymbol{u}$ is the displacement, $\boldsymbol{g}$ and $\boldsymbol{h}$ are refered as essential, Dirichlet, and natural, Neumann boundary condition, respectively. Here we consider a finite deformation analysis, where the deformation map $\boldsymbol{\phi}$, $\boldsymbol{x} = \boldsymbol{\phi}(\boldsymbol{X})$, describes the motion of each materail particle from its initial reference configuration $\boldsymbol{X}$ to its deformed configuration $\boldsymbol{x}$. The displacement field $\boldsymbol{u}$ and the deformation gradient $\boldsymbol{F}$ follow as

$$\boldsymbol{u} = \boldsymbol{x} - \boldsymbol{X} \qquad \boldsymbol{F} = \frac{\partial \boldsymbol{x}}{\partial \boldsymbol{X}} \tag{2}$$

Also, the deformation gradient can be represented by the rotation tensor $\boldsymbol{R}$ and the spatial stretch tensor $\boldsymbol{V}$, $\boldsymbol{F} = \boldsymbol{V}\boldsymbol{R}$. Thus, $\boldsymbol{V}^2$ can be obtained from the left Cauchy-Green tensor

$$\boldsymbol{F}\boldsymbol{F}^T = (\boldsymbol{V}\boldsymbol{R})(\boldsymbol{R}^T\boldsymbol{V}) = \boldsymbol{V}^2 \tag{3}$$

The logarithmic strain tensor, denoted by $\boldsymbol{\epsilon}$, is computed as $\boldsymbol{\epsilon} = \ln\boldsymbol{V}$. The constitutive relationship, $\boldsymbol{\sigma} = \boldsymbol{\sigma}(\boldsymbol{\epsilon})$, is necessary to form a complete set of equations for computing the state variable, $\boldsymbol{u}$. Here we assume a linear isotropic relationship between logarithmic strain and the Kichhoff stress (see [9] for details of the finite deformation framework).

2.1. Discrete form

The continuum body Ω is discretised by finite set of N_p material points $\{\boldsymbol{x}_p\}_{p=1}^{N_p} \in \Omega$ in the original configuration that are tracked throughout the deformation process. Also, space is discretised by a background mesh defined by a set of N_n control points $\{\boldsymbol{x}_i\}_{i=1}^{N_n}$. The discrete MPM equilibrium equations are constructed by pre-multiplying the strong form of equilibrium (1) by a weighting function and applying integration by parts. A simple one-point quadrature rule is applied over each volume Ω_p associated with the pth material point to give

$$-\sum_{p=1}^{N_p}\left\{\Big(\boldsymbol{\sigma}(\boldsymbol{x}_p) : \nabla \boldsymbol{w}^h(\boldsymbol{x}_p)\Big)\Omega_p\right\} + \Big(\boldsymbol{h}, \boldsymbol{w}^h\Big)_{\Gamma_N} + \sum_{p=1}^{N_p}\left\{\Big(\boldsymbol{f}(\boldsymbol{x}_p) \cdot \boldsymbol{w}^h(\boldsymbol{x}_p)\Big)\Omega_p\right\} = \boldsymbol{0}. \tag{4}$$

(4) is solved on a finite dimensional space using functions represented in terms of B-spline basis functions, N_i^q. A B-spline basis is constructed from piece-wise polynomials joined with a prescribed continuity. In order to define a B-spline basis of polynomial order q in one dimension it is necessary to define a *knot vector*. A knot vector in one dimension is a set of non decreasing coordinates in the parametric space, written as

$$\Xi = \{0 = \xi_1, \xi_2, ..., \xi_{n+q+1} = 1\} \tag{5}$$

where $\xi_1 \leq \xi_2 \leq ...\xi_{q+n+1}$ and n is the total number of basis functions. Given Ξ and q, univariate B-spline basis functions are constructed recursively starting with piecewise

$$N_i^0(\xi) = \begin{cases} 1 \text{ if } \xi_i \leq \xi < \xi_{i+1} \\ 0 \text{ otherwise} \end{cases} \tag{6}$$

For $q = 1, 2, 3, ...$, they are defined by

$$N_i^q(\xi) = \frac{\xi - \xi_i}{\xi_{i+q} - \xi_i} N_i^{q-1}(\xi) + \frac{\xi_{i+q+1} - \xi}{\xi_{i+q+1} - \xi_{i+1}} N_{i+1}^{q-1}(\xi) \tag{7}$$

Note that when $\xi_{i+q} - \xi_i = 0$, $(\xi - \xi_i)/(\xi_{i+q} - \xi_i)$ should be vanished, and similarly, when $\xi_{i+q+1} - \xi_{i+1} = 0$, $(\xi_{i+q+1} - \xi)/(\xi_{i+q+1} - \xi_{i+1})$ is taken to be zero as well. These basis functions have the following properties: (i) they form a partition of unity, (ii) have local support and (iii) are non-negative (for more details see [10]). Fig. 1 shows

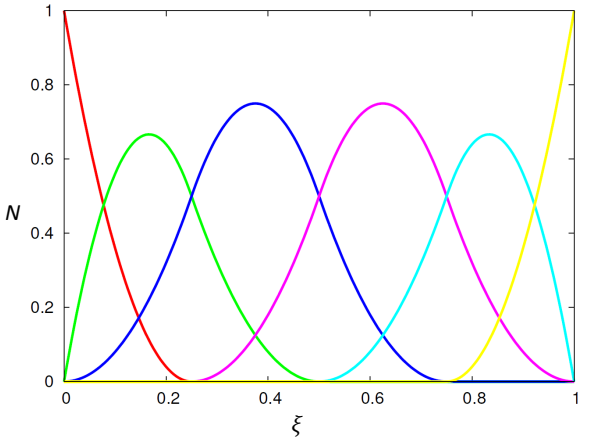

Fig. 1. Quadratic B-spline basis functions for four C^1-continuous elements with open knot vector, $\Xi = \{0, 0, 0, \frac{1}{4}, \frac{1}{2}, \frac{3}{4}, 1, 1, 1\}$.

quadratic B-spline basis functions for four C^1-continuous elements with open knot vector, $\Xi = \{0, 0, 0, \frac{1}{4}, \frac{1}{2}, \frac{3}{4}, 1, 1, 1\}$.

The explicit representation of $\boldsymbol{w}^h(\boldsymbol{x})$ in terms of the basis functions and control variables is assumed to take the standard form

$$\boldsymbol{w}^h(\boldsymbol{x}) = \sum_{i=1}^{N_n} N_i^q \boldsymbol{w}_i(\boldsymbol{x}). \tag{8}$$

Substituting the weighting function approximation into (4) and after simplification, the discrete MPM equation is obtained as

$$-\sum_{p=1}^{N_p} \left\{ \Big(\boldsymbol{\sigma}(\boldsymbol{x}_p) \cdot \nabla N_i^q(\boldsymbol{x}_p) \Big) \Omega_p \right\} + \int_{\Gamma_N} \boldsymbol{h} N_i^q d\Gamma + \sum_{p=1}^{N_p} \left\{ \boldsymbol{f}(\boldsymbol{x}_p) N_i^q(\boldsymbol{x}_p) \Omega_p \right\} = \boldsymbol{0}. \tag{9}$$

The numerical solution of this quasi-static problem is typically obtained in steps by incrementally imposing displacement boundary conditions, external forces or both in order to obtain increment in displacement, $\Delta \boldsymbol{u}$. Here a fully

implicit method is employed to solve the problem. Once the displacement increment is obtained, the material point position, $\boldsymbol{x}_p$, and displacement, $\boldsymbol{u}_p$, are updated as follows

$$\boldsymbol{x}_p^{k+1} = \boldsymbol{x}_p^k + \sum_{i=1}^{N_n} \Delta \boldsymbol{u}_i N_i^q(\boldsymbol{x}_p^k) \qquad \text{and} \qquad \boldsymbol{u}_p^{k+1} = \boldsymbol{u}_p^k + \sum_{i=1}^{N_n} \Delta \boldsymbol{u}_i N_i^q(\boldsymbol{x}_p^k), \tag{10}$$

where k denotes the loadstep number. After each load step, the spatial position of background grid is reset to its original undeformed state.

3. Numerical results

Here we present the numerical results for a one-dimensional elastic column quasi-statically compressed by its own weight through the application of a body force, b_f, per unit mass. The initial material density, $\rho_0 = 1$, Young's modulus $E = 10^6$, and initial column height $L_0 = 50$, all in compatible units. The column initially occupies 50 elements and the body force was applied over 20 loadsteps. This one-dimensional problem has a semi-analytical solution described below. The Cauchy strees is obtained from the initial position within the column, X, that is

$$\sigma = \rho_0 b_f (L_0 - X) \tag{11}$$

The utilised finite deformation framework makes use of a linear relationship between logarithmic strain and Kirchhoff stress, τ. The Cauchy and Kirchhoffstresses are linked through, $\sigma = \frac{\tau}{J}$, where the $J = \det(F)$ and $F = \partial x/\partial X$ is the deformation gradient, x is the updated position in one-dimension $\det(F) = F$. In one dimension the logarithmic strain is defined as

$$\epsilon^{(0)} = \frac{1}{2}\ln(F^2) = \ln(F) \tag{12}$$

and we assume that the Kirchhoff stress is linked to the logarithmic strain through

$$\tau = E\epsilon^{(0)} \tag{13}$$

combinig the equations (12) and (13) the Cauchy stress is expressed as

$$\sigma = \frac{1}{F} E \ln(F). \tag{14}$$

By using equation (11), σ can be obtained for any point in the problem domain and then we can solve for the deformation gradient using a Newton method.

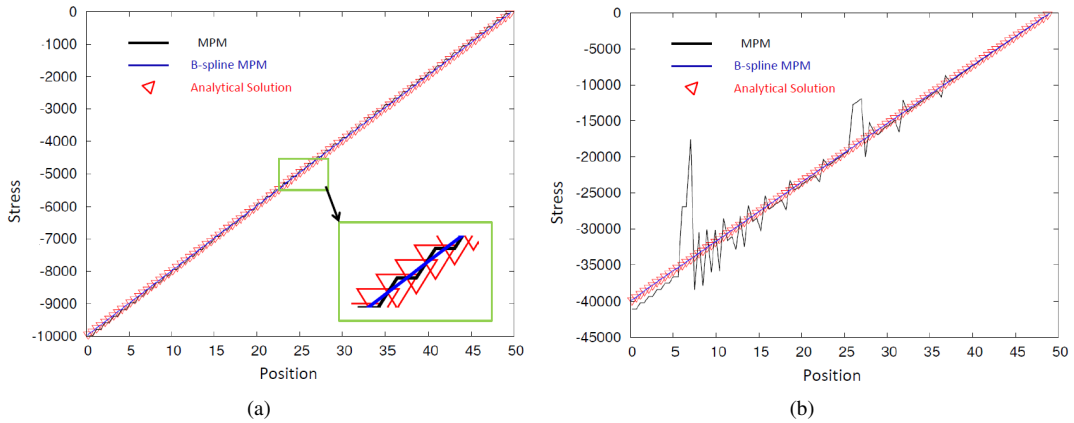

Fig. 2. Numerical and analytical solutions to the one-dimensional elastic column quasi-statically compressed by its own weight under a body force for (a) W=10000; (b) W=400000.

Fig. 2 shows the stress distribution with $b_f = -200$ and $b_f = -800$, that is with a total column weight of $W = \rho_0|b_f|L_0 = 10000$ and $W = 40000$, respectively. Results are shown for the standard MPM with linear basis functions and for the cubic B-spline MPM ($q = 3$) and compared against the semi-analytical solution. For the MPM the problem is initially discretised with one particle per grid cell as, for this very simple problem, increasing the number of material points reduces the accuracy of the simulation. The B-spline MPM used four particles per grid cell. Although for $b_f = -200$ both the methods provide a reasonable approximation to the semi-analytical solution, MPM still shows small osillations. However, for $b_f = -800$ spurious oscillations can be seen in the MPM results caused by cell-cross instabilities whereas the B-spline MPM removed the oscillations.

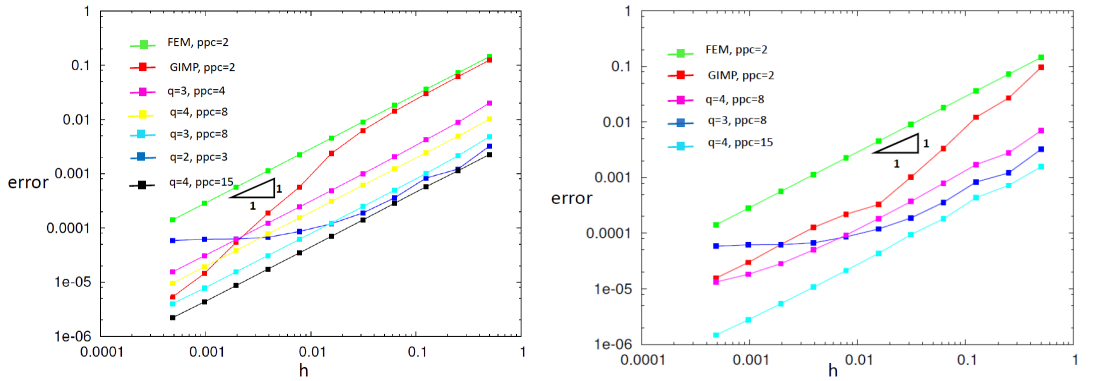

Fig. 3. Convergence of stress calculated by B-spline MPM, GIMP and linear FEM for (a) W=10000; (b) W=400000.

Fig. 3 displays the errors in the simulations based on the following error measure and the semi-analytical solution at the current particle locations

$$\text{error} = \sum_{p=1}^{N_p} \frac{V_p^0|\sigma_p - \sigma_A(X_p)|}{WL_0} \tag{15}$$

X_p is the particle original location, V_p^0 is the original volume associated with the material point, σ_p is the material point stress and $\sigma_A(X_p)$ is the semi-analytical stress.

The error comparison of B-spline MPM for quadratic (q=2), cubic (q=3) and quartic (q=4) basis functions with GIMP and linear FEM has been shown in Fig.3-a. The total column weight, W, is 10000. On the coarse mesh, quadratic B-spline MPM represents less error compare to cubic and quartic (with ppc=8) B-spline MPM as well as GIMP whereas the fine grids give us the smaller errors for quartic and cubic than quadratic B-spline MPM and even GIMP provides a better result than quadratic B-spline MPM. When we are dealing with small deformation (e.g. W = 10000), cell-cross instabilities are not too severe particularly on the coarse meshes, therefore quadratic B-spline gives a very good result while on the fine meshes cubic and quartic B-spline show more promising results. One reason for this is the compact support of B-spline basis functions. By increasing the compact support of basis functions, the effect of cell-crossing problem is reduced. This can be achieved by increasing the order of B-spline basis functions.Fig.3-b shows the error of simulation for a W=400000 for FEM with linear elements as well as GIMP and B-spline MPM. As it has been shown in the Fig.3-a and Fig.3-b, the optimum rates of convergence were not achieved due to projection and integration errors. Note that these errors can be reduced by using data reconstruction approaches, such as Moving Least Square (MLS) technique [11].

4. Conclusions

This paper has presented a MPM where the standard linear basis functions have been replaced by B-splines. The higher order smoothness of the splines significantly improves the accuracy of the method by removing the cell-cross

instabilities seen in other MPMs however the optimum convergence rates have not been achieved due to projection and integration errors.

Acknowledgements

The authors acknowledge the support of EPSRC grant EP/M017494/1.

References

[1] F. Harlow. Hydrodyanamics problems involving large fluid distortions, J. Assoc. Compos. Mach. 4 (1957) 137–142.
[2] M. Evans, F. Harlow. The particle-in-cell method for hydrodynamic calculations, Tech. Rep. LA-2139, Los Alamos Sci. Lab., Los Alamos, N. M., 1957.
[3] J. U. Brackbill, H. M. Ruppel. Flip: A method for adaptively zoned, particle-in-cell calculations in two dimensions, J. Comput. Phys. 65 (1986) 314–343.
[4] D. Sulsky, Z. Chen, H. L. Schreyer. A particle method for history-dependent materials, Comput. Methods Appl. Mech. Eng. 118 (1994) 179–196.
[5] D. Sulsky, S. J. Zhou, H. L. Schreyer. Application of a particle-in-cell method to solid mechanics, Comput. Phys. Commun. 87 (1995) 236–252.
[6] D. Sulsky, H. L. Schreyer. Axisymmetric form of the material point method with applications to upsetting and Taylor impact problems, Comput. Methods Appl. Mech. Eng. 139 (1996) 409–429.
[7] S. Bardenhagen, E. Kober. The generalized interpolation material point method, CMES-Computer Modeling in Engineering and Sciences 5 (2004) 477–495.
[8] A. Sadeghirad, R. M. Brannon, J. Burghardt. A convected particle domain interpolation technique to extend applicability of the material point method for problems involving massive deformations, Int. J. Numer. Meth. Engng. 86 (2011) 1435–1456.
[9] W.M. Coombs, Finite deformation of particulate geomaterials: frictional and anisotropic Critical State elasto-plasticity, Ph.D. thesis, Durham University, 2011.
[10] L. Piegl, W. Tiller, The NURBS Book (Monographs in Visual Communication), 2nd Edition., Springer-Verlag, New York, 1997.
[11] D. Sulsky, M. Gong, Improving the Material-Point Method, Innovative Numerical Approaches for Multi-Field and Multi-Scale Problems.(2016) 217–240.